Progress toward the Development of a Single Molecule Transistor with Graphene Electrodes

Thesis by
Emma Rose Schmidgall

In Partial Fulfillment of the Requirements
for the Degree of
Bachelor of Science

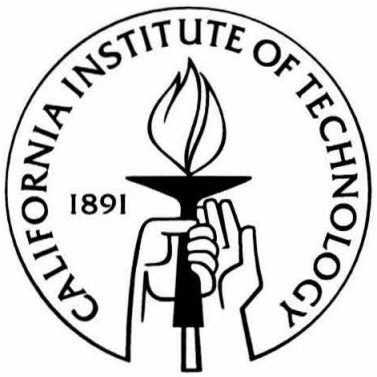

California Institute of Technology
Pasadena, California

2007
(Submitted May 1, 2007)

Acknowledgements

I would first and foremost like to acknowledge my advisor, Professor Marc Bockrath, and my co-advisor, Mr. Brian Standley, for their assistance with this project, for teaching me the necessary research techniques, and for encouraging me to explore new ideas. It has been a pleasure working with you.

I would also like to acknowledge the entire Bockrath Research Group for welcoming me into the lab for this past year. Vikram, Hsin-Ying, Jinseong, Hareem, Henk, Isabella and Megan: it has been a real pleasure!

I would like to acknowledge the Blacker Hovse Senior Physics Majors: Jeffrey Graham, Yuliya Kusnetsova, Emily Russell, and Klimka Szwaykowska. You've been with me at 2am working on Ph12b, 5:30 am working on Ph125, and through all of the physics good times and the physics bad times. Special thanks to those of you who repeatedly ended your recent conversations with me with, "Now, Emma...really...go write your thesis." Special thanks to Emily Russell for proofreading a draft of this thesis.

To my family – Mom, Dad, and Christina – for their support during four years of an intense Caltech education and all the school that lead here.

שחר שלי, תודה עצומה לך על התמיכה, העידוד, החיזוקים, כל האהבה ותיקוני המחשבים בשעת חירום.

Abstract

Single molecule transistors are useful for studying both the charge and spin states of molecules. These devices consist of a nanogap with three contacts for the source, drain, and gate. Current versions use metallic contacts for the source and drain, which remain essentially three-dimensional. It is thought that graphene contacts for the source and drain, which would be atomically flat, would enable the observation of more molecular charge states due to reduced screening between the sample and the contacts. This thesis presents the progress made in the development of graphene single molecule transistors during the 2006-2007 academic year. Additionally, this thesis will introduce a new method for the large-scale production of graphene samples.

Contents

Acknowledgements iii

Abstract v

1 Introduction 1

2 Fabrication of a Graphene Single Molecule Transistor 6

3 Measurements and Preliminary Data 18

4 A New Method for Making Graphene 24

5 Capacitive Properties of Graphene 31

6 Conclusions and Future Directions 36

Chapter 1

Introduction

Graphene, the name given to a single layer of graphite, is a two-dimensional carbon structure consisting of carbon atoms in a network of interconnected hexagonal rings. It shows promise as a material whose properties can be controlled through the application of an electric field. In 2004, Noveselov *et al.* demonstrated gate voltage-dependent changes in the conductivity of graphene [1]. Shortly thereafter, Zhang *et al.* observed the quantum Hall effect in this material [2]. Their experiment also suggested that the quantum Hall effect, as observed in graphene, is a half-integer effect. Further studies of the electrical conductivity of bilayer graphene suggest that a previously unknown variant of the integer quantum Hall effect, resulting from the interaction between the two graphene layers, is also present [3].

Previous single molecule transistors [4] have consisted of two closely spaced (1nm) gold electrodes on a Si/SiO_2 substrate and a voltage gate on the back of the device (Figure 1.1). A sample of interest, generally a single molecule or some other system consisting of only a few atoms, is placed between the electrodes through the application of a dilute solution of the subject molecules to the device. The solvent evaporates away and solute molecules are left behind on the substrate, hopefully between the two electrodes of the single molecule transistor. A gate voltage is applied to the sample, and current and voltage measurements can be made across the source and drain electrodes. The configuration of the energy states of the molecule can then be measured experimentally. Additionally, this technique allows

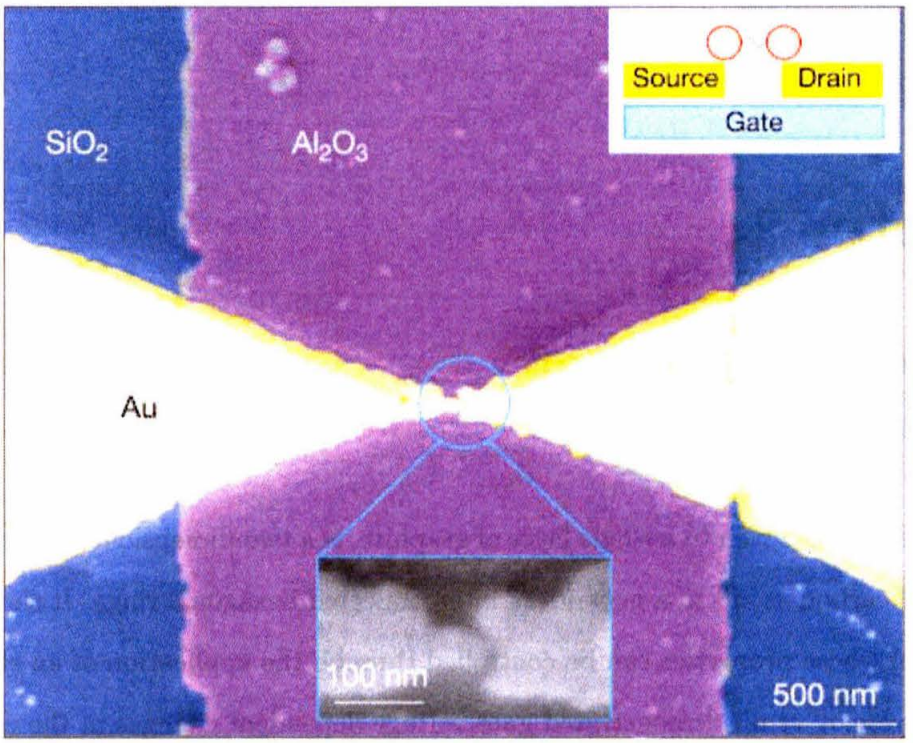

Figure 1.1: A single molecule transistor from [4]. The inset in the upper right is a schematic representation of a molecule in a single molecule transistor. The inset in the lower center is a magnified view of the nanogap.

for control of the sample spin state through the chemistry of spin impurities.

One interesting phenomenon that has been observed with single molecule transistors is the Kondo resonance [4]. In single molecule transistors, the Kondo resonance results from an exchange interaction between the localized spin on the sample molecule and electrons in the bulk metallic electrodes. This effect is most readily viewed as a peak in the differential conductance of a single molecule transistor containing a spin impurity when zero bias voltage is applied across the source and drain electrodes (Figure 1.2a). This peak disappears when the molecule is in a singlet spin state. Consequently, the Kondo peak may be present for some range of gate voltages and not for other ranges, depending upon what electronic and spin states are available in the analyte molecule. This is seen in the experiments presented

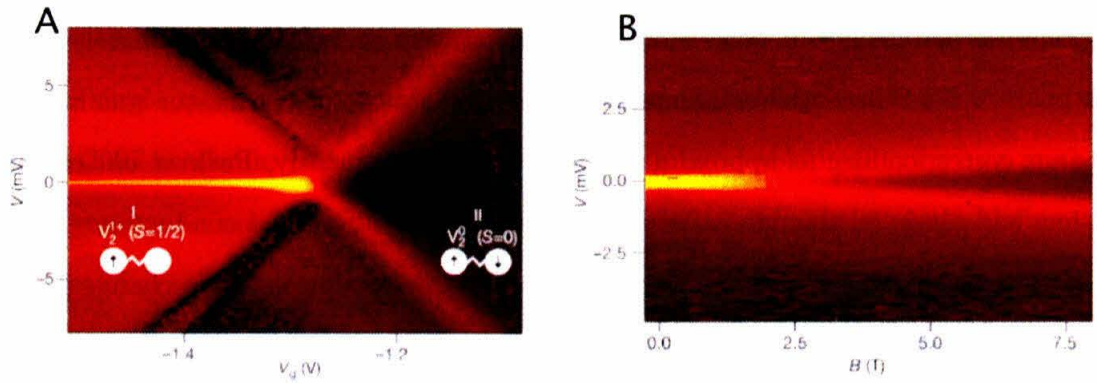

Figure 1.2: Differential conductance data from [4]. a) The Kondo resonance is clearly visible as a yellow peak at V= 0 on the left side of the image. The inset schematics represent the spin state of the molecule, and the Kondo resonance vanishes on the right side of the image when the molecule is in a singlet spin state. b) Differential conductance as a function of applied magnetic field for $V_g = -0.1$V and T=300mK. Note the splitting of the Kondo resonance peak as a function of magnetic field strength, displayed on the image x-axis.

in Liang *et al.* [4]. To verify that the observed peak was related to a Kondo resonance from nonzero spin, the sample was placed in a magnetic field and the differential conductance measured as function of applied bias voltage and magnetic field strength. The conductance peak was observed to split with magnitude $\frac{2g\mu_B B}{e}$ where $g = 2$ is the g factor of the molecule and μ_B is the Bohr magneton. This splitting is twice that which arises from the Zeeman effect and consistent with that expected for the Kondo resonance. Liang *et al.* also analyzed the magnitude of the differential conductance peak as a function of temperature, and the decrease in magnitude of this peak was consistent with that expected from the Kondo effect.

Single molecule transistors can also be used to study the vibrational modes of molecules and the interactions between these molecules and the substrate. Park *et al.* studied the behavior of C_{60} in a single molecule transistor system and were able to observe both an internal vibrational mode and an interaction between the molecule and the gold electrodes [5].

The observed C_{60} vibrational mode is the lowest-energy mode where the spherical molecule changes to a prolate ellipsoid. This mode has an excitation energy of approximately 33 meV, and a peak in the differential conductance of the single molecule transistor was noticed at an energy corresponding to approximately 35 meV. Consequently, Park *et al.* concluded that they had observed this vibrational mode. A peak in differential conductance was also noticed at 5 meV. Park *et al.* hypothesized that this peak represented a change in center of mass separation between the C_{60} molecule and the gold electrodes. When an electron is added to C_{60}, an interaction between that electron and the image charge in the gold electrode pulls the C_{60} closer to the Au surface, decreasing the center of mass separation. Conversely, when an electron is removed, the center of mass distance increases due to the absence of this electron/image charge interaction. Numerical models assuming a Lennard-Jones potential for the C_{60}/Au interaction suggest that the energy involved in changing this center of mass distance is on the order of 5 meV. The results of the Park *et al.* experiment indicate that single molecule transistors can be used to study vibrational and rotational energy states in addition to electronic properties.

It is thought that graphene nanogaps may be even better suited to single molecule transport experiments than the current gold electrode system because graphene is a two-dimensional conductor, while the metallic contacts of previous experiments are three-dimensional. This change in dimensionality could potentially result in the observation of more molecular charge states due to reduced screening between the analyte molecule and the contact electrodes. The dimensionality of graphene could also lead to interesting variations in the previously-observed Kondo effect, as this effect results from interactions between a localized spin impurity and the bulk. Therefore, changing the dimensionality of the bulk electrodes may change the observed Kondo behavior. Additionally, with the use of atomically flat contacts there is the potential to use scanning tunneling microscopy to verify the presence and position of the molecule in the nanogap, something which is not readily achievable with

metallic electrodes due to the depth of the nanogap in these materials.

The ultimate goal of this research is the development and successful demonstration of a graphene single molecule transistor. This paper presents the progress that was made during the 2006-2007 academic year, specifically emphasizing the development of a new method for making graphene samples in bulk. Results from a brief experiment studying the capacitive properties of graphene are also included.

Chapter 2

Fabrication of a Graphene Single Molecule Transistor

The graphene fabrication method used at the beginning of this project was a brute force method that involved cleaving a highly oriented pyrolytic graphite sample with Scotch tape and then rubbing this surface against the Si/SiO_2 substrate[6]. This procedure results in a few candidate single-layer graphene flakes per substrate. The number of single-layer flakes resulting from this procedure can be increased through a liftoff technique. Polydimethylsiloxane (PDMS) is an organic polymer which sticks slightly to the Si/SiO_2 substrate. Clean PDMS is applied to the sample surface, and larger graphite flakes will stick to the PDMS. When the PDMS is removed from the sample, these large graphite flakes are removed as well. Frequently, smaller single- or double-layered graphene flakes are found underneath larger graphite flakes. Consequently, PDMS liftoff increases the number of candidate graphene flakes on a given substrate.

It is also possible to derive single-layer graphene from Kish graphite, small flakes of highly oriented graphite. In this method, Kish graphite is first dipped in a 3:1 sulfuric acid/nitric acid solution and then baked for 3 minutes at 500 °C in Ar to separate the graphene layers. The material is deposited on an Si/SiO_2 substrate using dry sonication, and plasma cleaning with an oxygen plasma can be used to reduce the number of graphene layers present if most graphene samples on the Si/SiO_2 substrate are multilayer.

As a component of the research for this thesis, a method for fabricating graphene samples from the reduction of graphite oxide was developed. This method will be treated in Chapter 4. We will continue here with a discussion of the fabrication of nanogap devices after graphene deposition.

Optical microscopy can be used to identify candidate single-layer samples on an oxidized Si substrate. This is because the crystal layers of graphite change the optical path of reflected light with respect to light reflected from the empty SiO_2 substrate. The change in optical path resulting from even a single layer is substantial enough to be easily observed as a change in color, and the addition of multiple layers causes an even more significant color change [6]. The thinnest flakes appear light purple in color, and color varies through dark purple, blue, green, and gold as flake thickness increases. The color of flakes in an optical micrograph can thus be used to identify graphene candidates (Figure 2.1).

Atomic Force Microscopy (AFM) can be used to obtain a height measurement, relative to the substrate, for the candidate graphene flakes identified in light microscopy. AFM is a technique that can provide topographic information about a sample. A cantilever with a fine tip at the end, similar to the needle on a record player, is driven near its natural resonance frequency. A laser is reflected off the cantilever just above the tip, and the position of the reflected beam is detected by an array of photodiodes. Interaction with the sample surface changes the vibration of the tip, and these changes in amplitude and phase are used to reconstruct the topography of the sample surface. It was initially thought that only flakes with a measured height of less than 1nm relative to the substrate were candidate single-layer flakes, and this was consequently used as the AFM screening criterion.

A more accurate technique for identifying single-layer graphene flakes is Raman spectroscopy, which is a technique generally used to determine the type and nature of chemical bonds present in a sample. In this technique, a sample is illuminated with laser light and the shift in wavelength between the incident laser light and the reflected light yields information

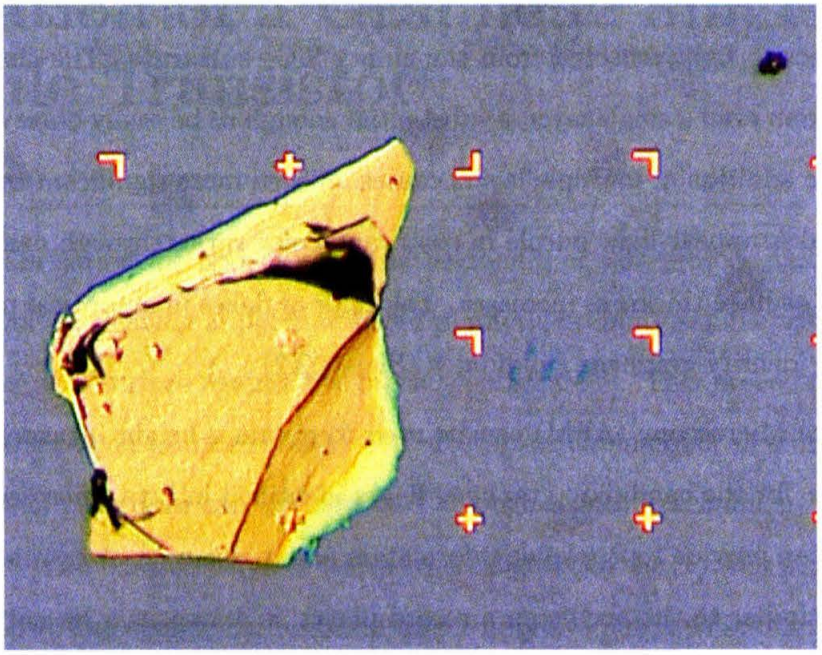

Figure 2.1: A light micrograph of graphene and graphite flakes on an Si substrate. Note the difference in color between the larger graphite flake on the left (gold) and the smaller graphene flakes on the right (blue-purple). This large graphite flake would be a candidate for liftoff with PDMS.

Site	AFM Height	AFM Number of Layers	Raman Number of Layers
1	1.07 ± 0.27 nm	1-2	1
2	1.70 ± 0.22 nm	3-4	1
3	1.29 ± 0.33 nm	2-3	2

Table 2.1: AFM and Raman spectroscopy data for the flake in Figure 2.3.

about the vibrational states of molecules and bonds in the sample. This change in energy is referred to as the Raman shift. For graphene, the Raman shift is a function of the number of layers present in the sample (Figure 2.2) [7].

We sent one of our graphene samples for analysis at the laboratory of Professor A. Ferrari at the University of Cambridge. Figure 2.3 shows the candidate flake and Table 2.1 includes the AFM-measured heights for each region, with our prediction of the number of layers present. The results of the Raman spectroscopy measurements are also included in Table 2.1.

The results of this Raman spectroscopy experiment suggest that our earlier AFM screening criterion was incorrect. Regions with a height larger than 1nm can possibly be single-layer and regions with a height of around 1nm where creases and ridges appear present in the AFM image represent multi-layer graphene. Consequently, we refined the AFM screening criterion to include as candidate single-layer graphene all flakes with a measured AFM height of less than 2nm with no ridges or creases visible in the image. This variation of the height of single-layer graphene across a sample suggests also that there may be some interaction between the graphene and the substrate that causes the graphene flakes to deposit unevenly.

Once candidate single-layer graphene has been identified optically and confirmed with AFM, electrodes contacting the candidate flakes are designed in an AutoCAD system. Occasionally, scanning electron microscopy (SEM) is used to obtain guide images for this process. These images show the position of the graphene flakes relative to a system of alignment

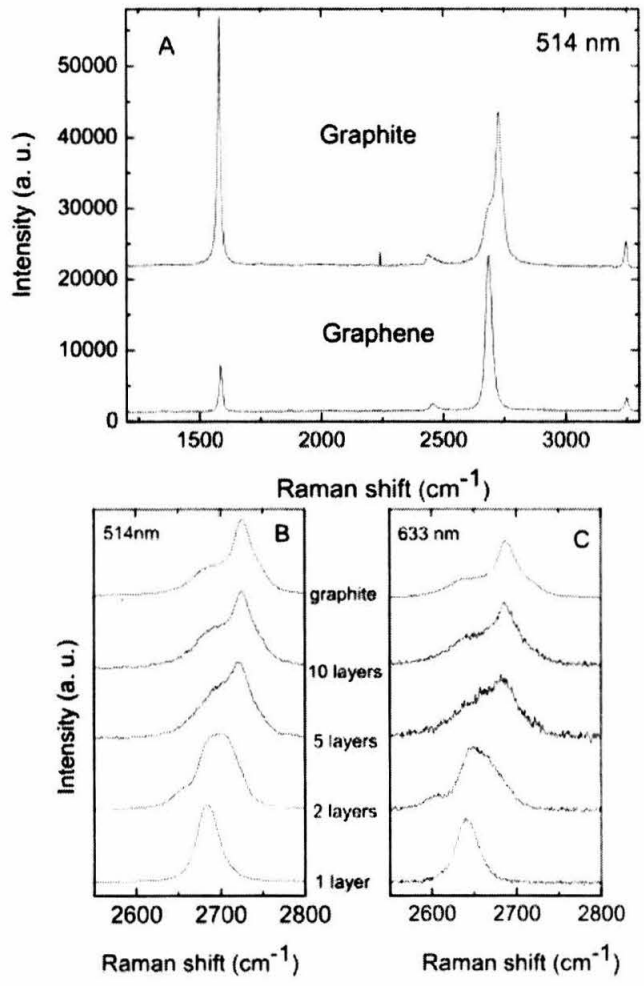

Figure 2.2: a) The Raman spectroscopic signatures of graphite and graphene. b,c) Raman shift as a function of the number of graphene layers present. [7]

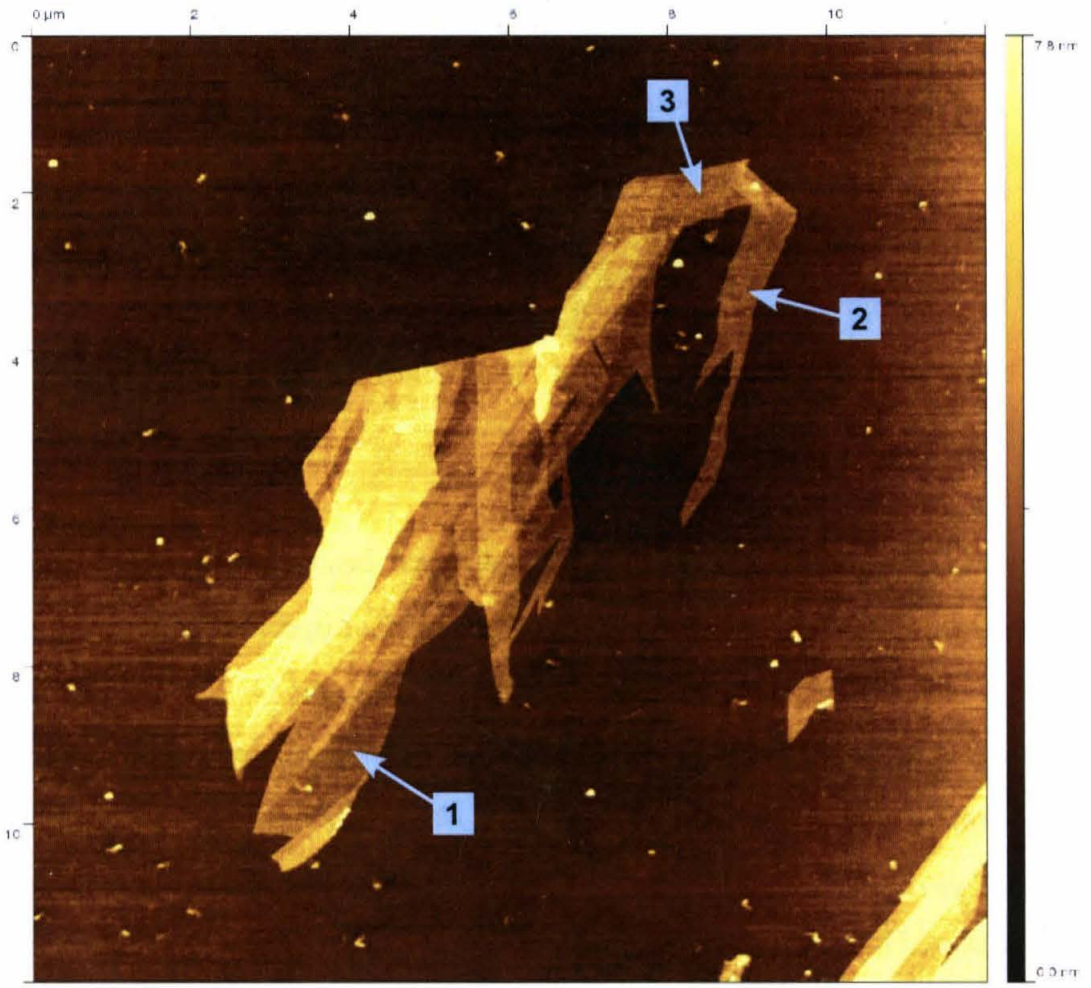

Figure 2.3: An AFM image of a candidate graphene flake. Suspected single-layer regions are indicated and numbered. Numbers correspond to those in Table 2.1

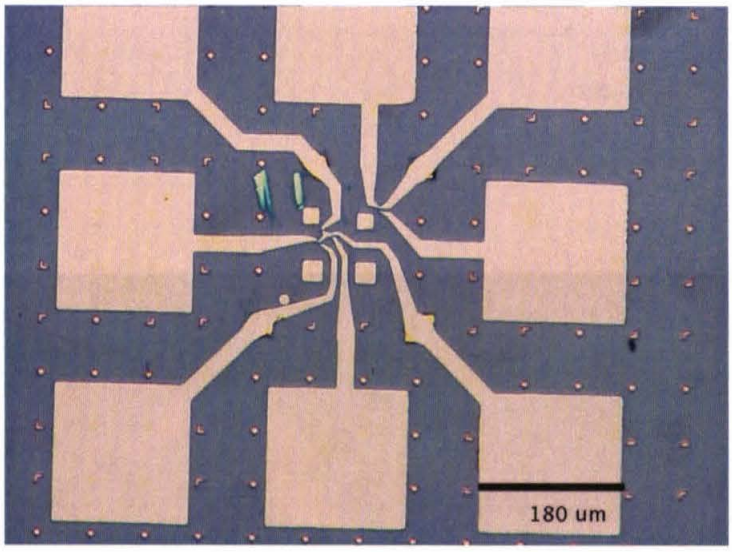

Figure 2.4: The electrodes and bond pads contacting a graphene flake.

marks previously evaporated onto the substrate. E-beam lithography is used to define the position and shape of electrodes on the sample. The sample is coated in an electron-sensitive positive resist, and a SEM electron beam is used to expose the resist in the pattern programmed into the AutoCAD file. The exposed resist is dissolved, and the sample is placed in a thermal evaporator where metal (Cr/Au) electrodes and bond pads are evaporated onto the graphene flake. Figure 2.4 shows the electrodes and bond pads for a graphene device. The sample is placed in a chip holder and attached to the conductive holder with silver paint. Fine wires connecting the pins of the chip holder to the bond pads are added with the aid of a wire bonder, and a gate voltage is applied through connecting the conductive sample holder and attached Si substrate to one of the pins of the chip holder. Figure 2.5 shows a device after wire bonding. At this point, voltages can be applied to the graphene flake and the gate.

The next step in device fabrication is the formation of a graphene nanogap. To form nanogaps in graphene, a voltage ramp is applied across the source and drain electrodes,

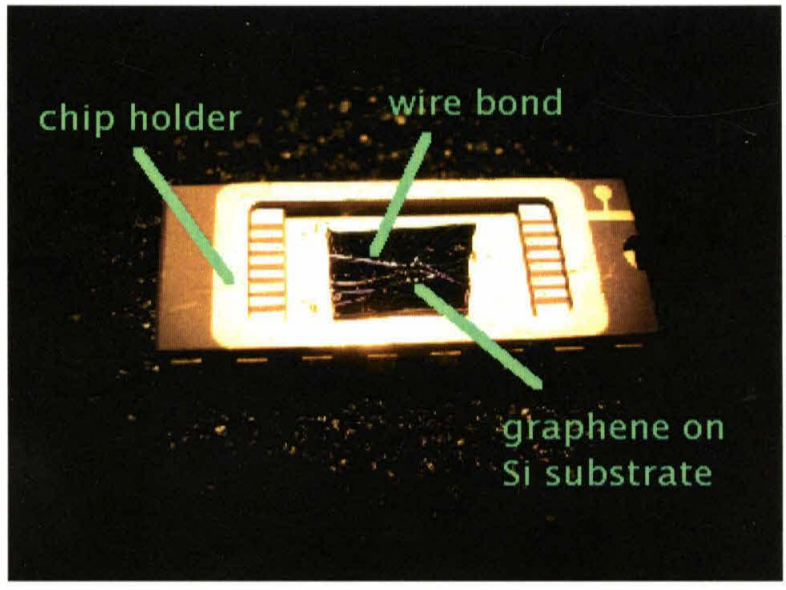

Figure 2.5: A graphene sample after wirebonding to the chip holder.

with the gate voltage set at zero. The current through the device is measured as voltage is increased. At first, current will increase roughly linearly with voltage. However, after a critical voltage has been applied, carbon atoms in the graphene will migrate with the applied voltage, and the current through the source and drain electrodes will drop rapidly. At this point, the applied voltage is ramped back to zero. Figure 2.6 shows the applied voltage, measured current, and measured conductivity for a representative nanogap formation. Figure 2.7 shows a nanogap formed from this method.

It is possible for the breakdown process to result in fairly straight and narrow gaps, as shown in Figure 2.7. However, it is also possible for the same breakdown process to result in gaps that are neither straight nor narrow, such as the example shown in Figure 2.8. Various methods for improved control over the breakdown process have been tried, such as performing breakdown with the device at low temperatures or performing the breakdown in an inert gas such as Ar. The latter method seems to show a little improvement, but this method has only been applied on a few samples. This is an area of ongoing research.

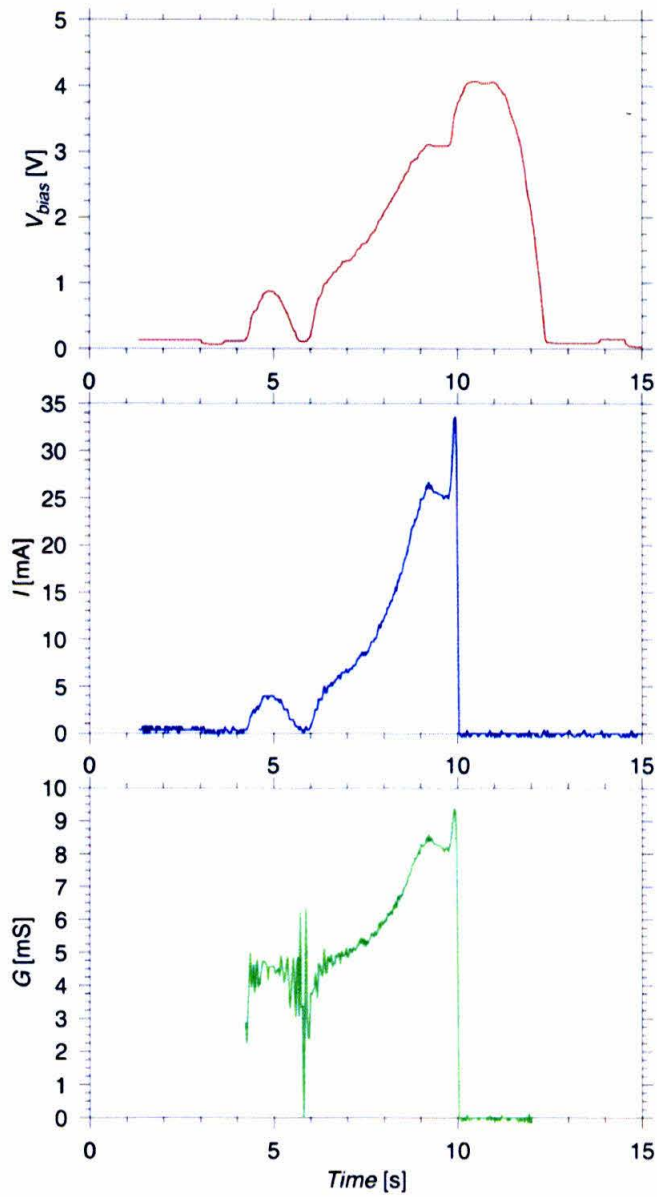

Figure 2.6: A plot of the applied voltage (top), current (center), and conductance (bottom) for a representative breakdown. Note the rough proportionality between current and voltage prior to breakdown.

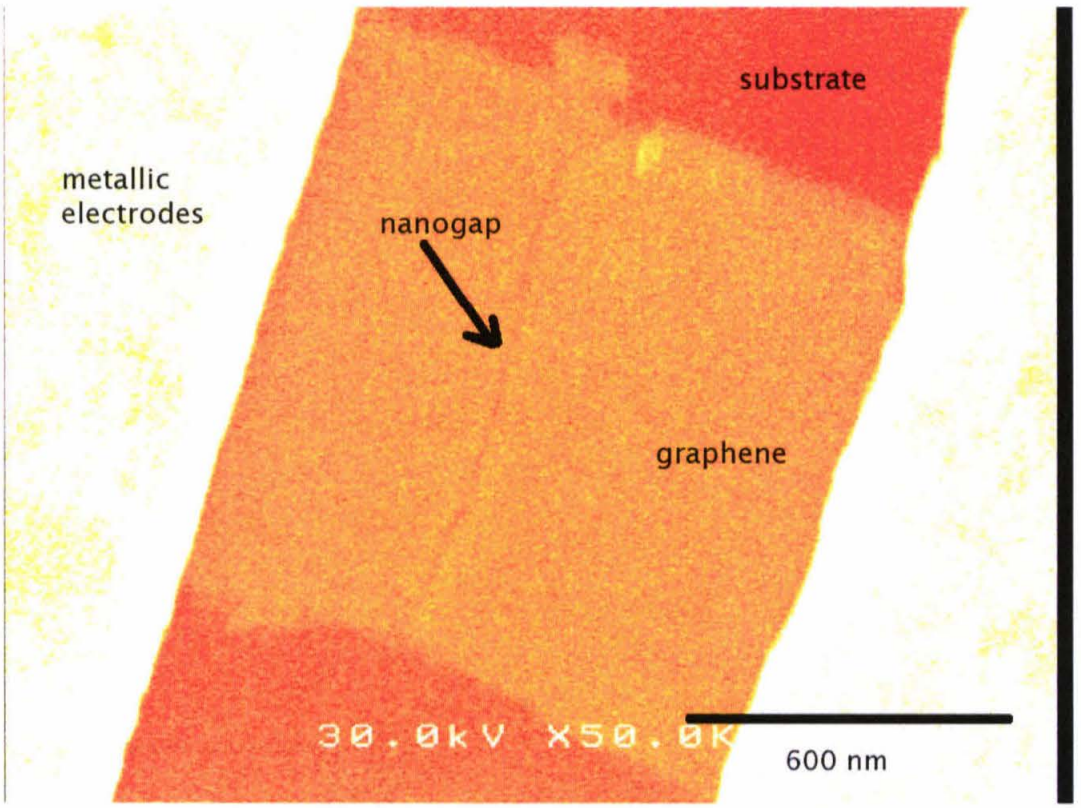

Figure 2.7: A straight and narrow nanogap formed by the breakdown process.

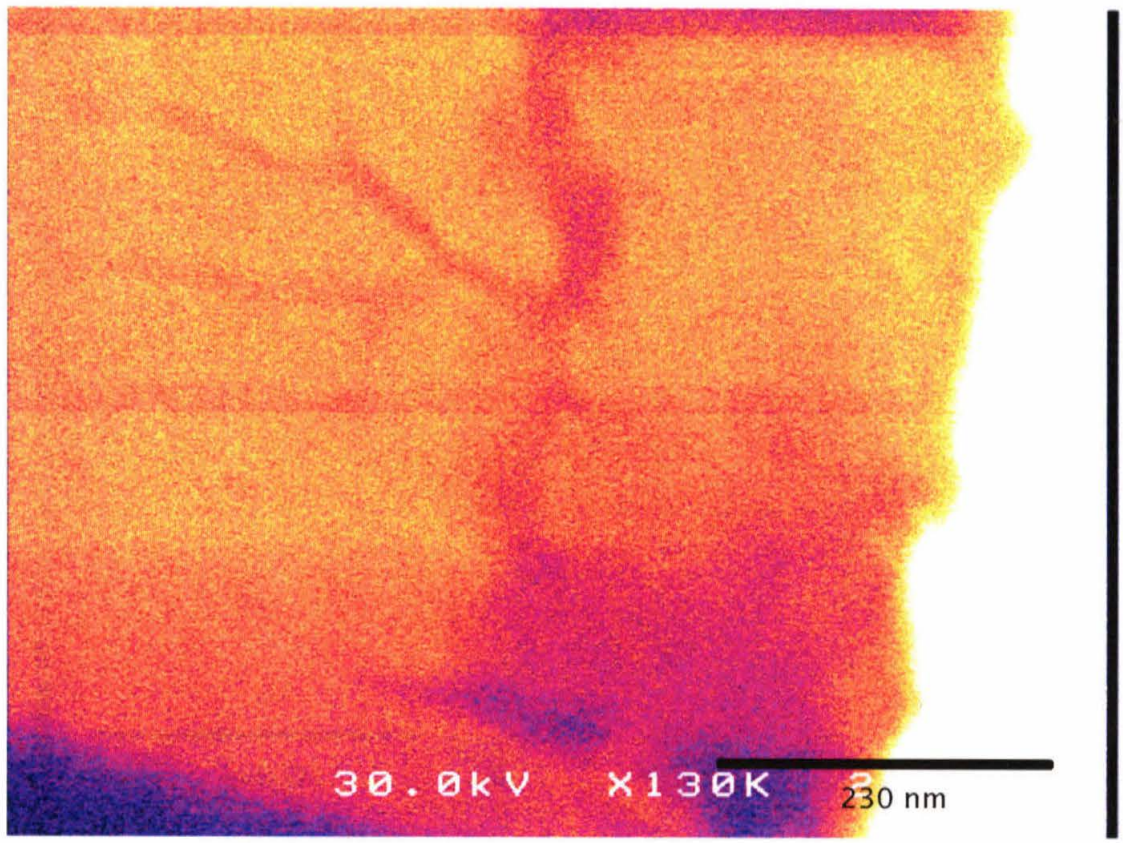

Figure 2.8: A gap that is neither straight nor narrow formed by the breakdown process.

Molecules are added to the device by applying a very dilute solution of the subject molecule to the device. When the solvent evaporates, the electronic characteristics of the device are tested to determine if a molecule is present in the nanogap (Chapter 3). A variation of this method involves applying the solution to the device first and then performing the nanogap breakdown. Both methods are currently used in the laboratory. With the addition of molecules to the graphene nanogap, we should now have a functional single molecule transistor. A few samples have successfully made it to this point. The following chapter will discuss preliminary measurements with these samples.

Chapter 3

Measurements and Preliminary Data

We are interested in measuring the electrical conductance properties of the nanogap and nanogap-molecule combinations. To this end, we measure current as both a function of source-drain bias voltage and gate voltage. These measurements can be performed at room temperature in the laboratory with the use of a National Instruments DAQ or a standard power supply as a voltage source. Current through the nanogap is, in all cases, amplified with a current amplifier and then measured with the National Instruments DAQ and lab-built data acquisition program, MeazureIt.

For empty nanogaps, devices where no analyte molecules have been applied, measurements are useful for determining the characteristics of the tunnel current through the nanogap. Figure 3.1 presents a standard tunneling current-voltage graph and the gate voltage dependence of the tunneling current is shown in Figure 3.2. Typically, the magnitude of the tunneling current is on the order of nanoamperes at both room temperature and 1.5 K. Note the absence of any significant gate voltage dependence in the behavior of the device tunneling current.

When molecules are present, the behavior of the device should change substantially as a function of gate voltage. Specifically, it should be possible to see effects of Coulomb blockades in the gate voltage dependence of the device current-voltage curves. For electrons to move through the nanogap, their final state at the drain electrode must be lower in energy

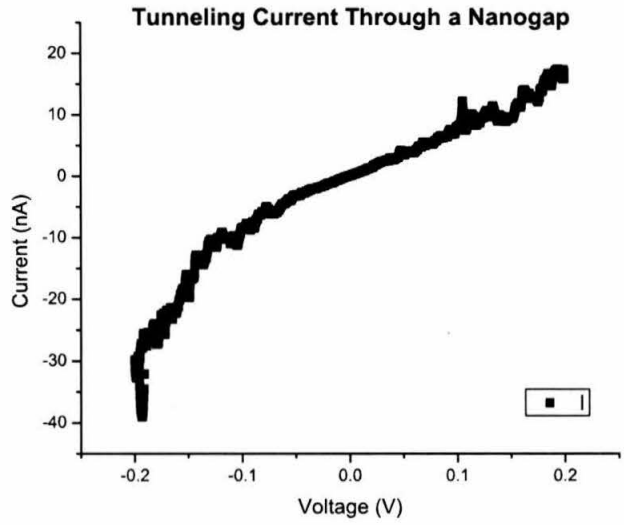

Figure 3.1: Tunneling current through a nanogap.

than their initial state at the source electrode (Figure 3.3). The molecule in between these two electrodes has a discrete energy spectrum consisting of various molecular orbital energy levels. The gate voltage changes the energy of these molecular orbital energy levels relative to the source and drain electrode energy levels. It is possible for electrons to move through the device one by one only when each successive state is lower in energy than the previous state, and the discrete energy levels of the molecule mean that there will be gate voltages for which electrons cannot travel through the device. The conditions for which tunneling occurs can be expressed as

$$\frac{-e}{2} \mp [en + (C_g + C_2)V_a - C_g V_g'] > 0 \tag{3.1}$$

and

$$\frac{-e}{2} \pm [en - C_1 V_a - C_g V_g'] > 0 \tag{3.2}$$

where $n \in \mathbb{N}$, C_g is the capacitance of the gate voltage contact, C_i is the contact capaci-

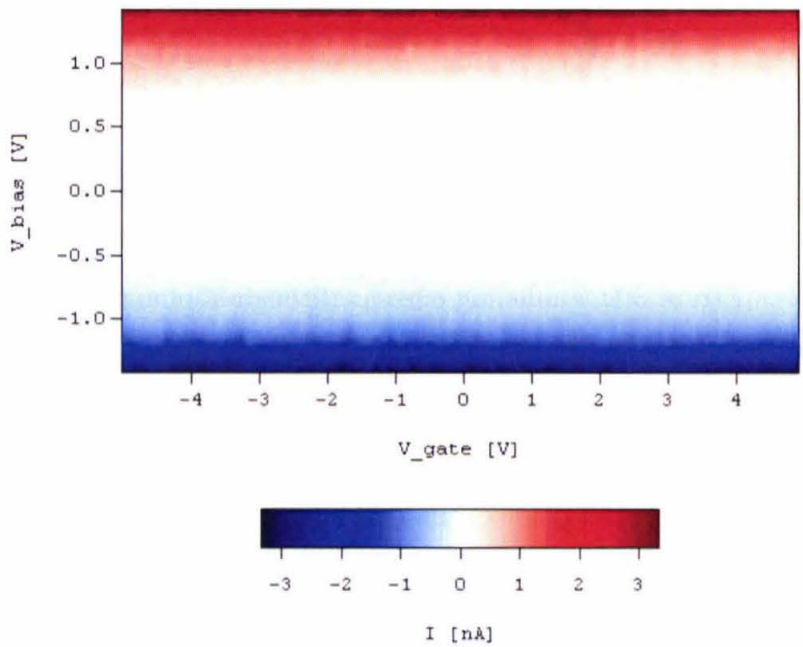

Figure 3.2: The gate voltage dependence of the tunneling current in a representative device. Gate voltage is on the horizontal axis and bias voltage is on the vertical axis. Current is represented in the color scale. Note the absence of any substantial gate voltage dependence.

tance of the source ($i = 1$) and drain ($i = 2$) electrodes, V_a is the applied bias voltage, and $V_g' = V_g + \frac{Q_p}{C_g}$ where V_g is the applied gate voltage and Q_p represents background polarization charge resulting from workfunction differences and random charges trapped near the junctions between the different materials in the transistor [13]. Both Equation 3.1 and Equation 3.2 are linear and, plotted in the bias voltage-gate voltage plane, form diamond-shaped regions inside which the device will not conduct. These are referred to as Coulomb diamonds (Figure 3.4) and should be present if there is a molecule in the nanogap.

Figure 3.5 presents data from a device with 9,10-dinitroanthracene applied as an analyte molecule. This image appears to contain candidate Coulomb diamonds. However, these Coulomb diamonds are not very clear and therefore we cannot say for certain that these devices contained molecules. Currently, we are trying this experiment again with C_{60} as this was the molecule used in previous experiments [4].

Once we are certain that a device contains molecules, the next step would be to consider the differential conductance of this device and look for variations between the Kondo physics observed with these devices versus the the gold single molecule transistors. Another extension would be to actually confirm the presence of an analyte molecule in the gap through the use of scanning tunneling microscopy.

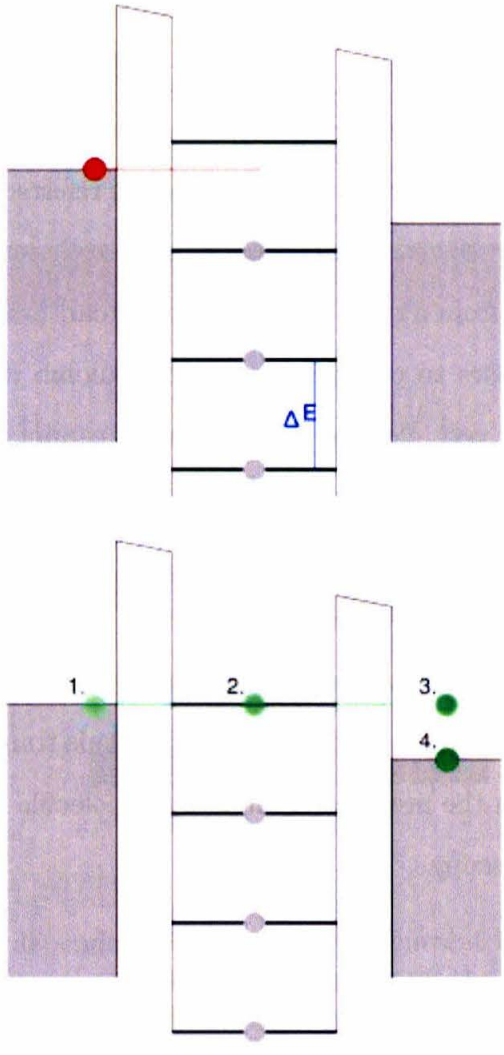

Figure 3.3: The blocks on the left and right of each image schematically represent the energy levels of the electrodes, and the ladder in the middle represents the molecular energy levels. The top image illustrates a case where an electron (red) cannot tunnel through the device. The lower image illustrates a case where the electron (green) can tunnel through the device. [12]

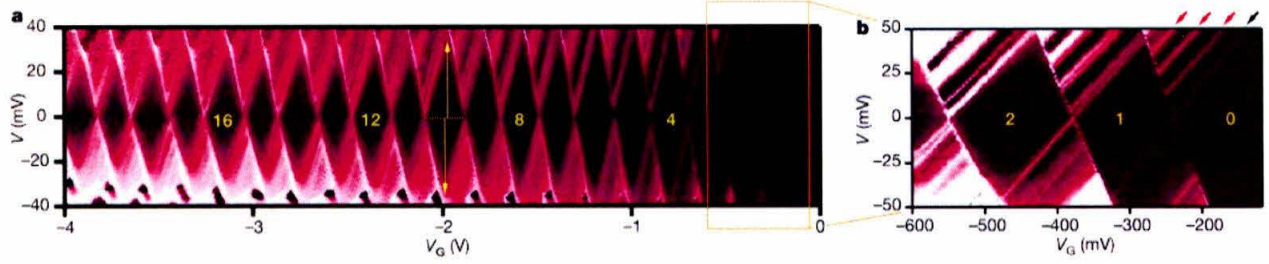

Figure 3.4: Coulomb diamonds clearly visible in these data from [14]. The differential conductance is displayed in the color scale, where black is zero and white is 3μS.

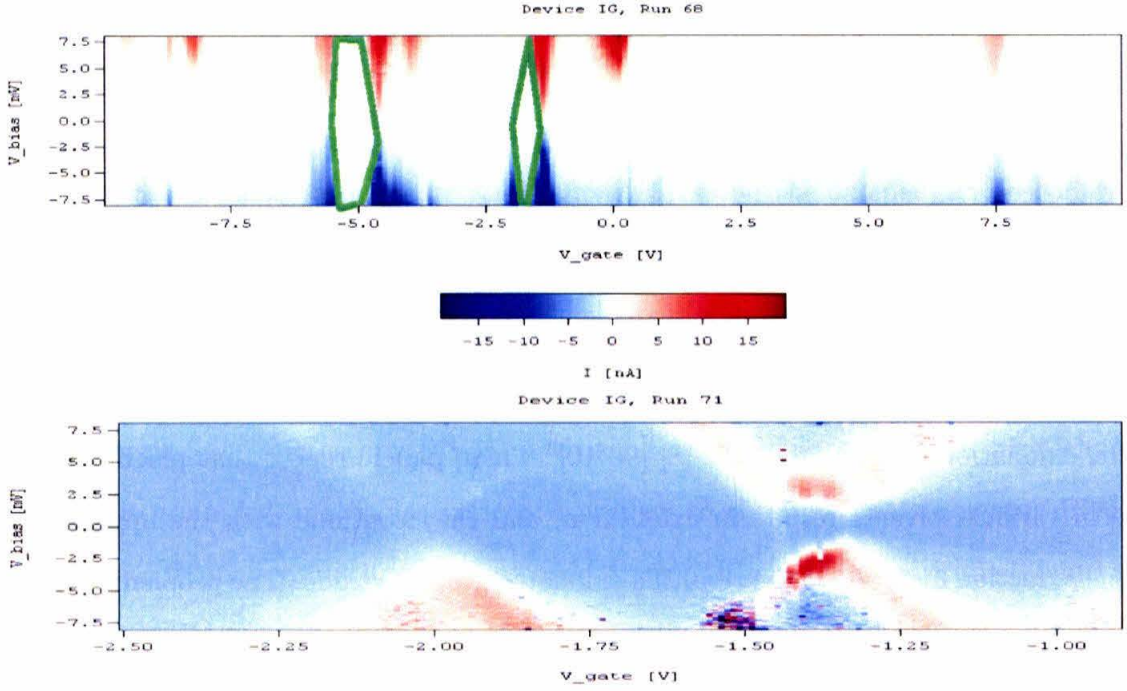

Figure 3.5: Data from a single molecule transistor with graphene electrodes. Candidate Coulomb diamonds are indicated in the upper image with green lines, and the lower image shows a close-up view of the candidate Coulomb diamond at -1.75V gate voltage. These data do not show a regular Coulomb diamond pattern and are therefore inconclusive. They may indicate the presence of more than one quantum dot in series or in parallel.

Chapter 4

A New Method for Making Graphene

One of the major issues in the development of these graphene single molecule transistors is the absence of a high-throughput method for producing graphene. Both the rubbing/liftoff method and the Kish graphite method result in only one or two usable candidate graphene samples per Si substrate, a rate substantially too low to produce large quantities of single molecule transistor devices given the failure rate of the nanogap breakdown process. Due to this slow rate of graphene production, it became necessary to investigate alternative methods for making this material.

Several recent papers have reported on the production of single-layer graphene samples via the exfoliation of graphite oxide [8] [9] [10]. These papers report that placing graphite oxide in various solvents results in exfoliation, and they continue with the application of various reduction methods to the resulting exfoliated graphite oxide. The problem with these papers is that the authors are generally attempting to produce functionalized graphene or polymer-coated nanoplatelets of graphene. Consequently, their reduction techniques are not in general suited for application to graphene single molecule transistors where the desired material is strictly graphene. However, through the new combination of a few techniques found across these papers, it appears to be possible to produce large quantities of single-layer graphene in the laboratory.

The first step in this process is to manufacture graphite oxide in the laboratory. A

chemical reaction for oxidizing graphite was published by Hummers in the 1950s [11]. This reaction involves combining powdered flake graphite, sulfuric acid, sodium nitrate, and potassium permanganate. The graphite oxide is then separated from the solution through the use of a standard filtration technique, and rinsed thoroughly to remove any dissolved salts. The resulting filtrate is then mixed with deionized water to a total volume of approximately 50 mL. This solution is then diluted to about one part per thousand in deionized H_2O.

Since graphite oxide is readily exfoliated in water [9], this dilute solution of graphite oxide is placed in an ultrasonic mixer for an hour. After the ultrasonication, the graphite oxide layers should be completely exfoliated. This solution is then deposited on a Si/SiO_2 substrate drop by drop, and the water is allowed to evaporate completely between drops, with evaporation accelerated using a hot plate. After about four repetitions of this process, the graphite oxide sheets are dense enough to be barely visible in an optical microscope. With AFM, the presence of graphite oxide single sheets on the sample can be confirmed. Figure 4.1a shows an AFM micrograph of graphite oxide on a Si/SiO_2 substrate. Most of the flakes visible in the image have measured heights of approximately a nanometer relative to the substrate.

Electrostatic force microscopy (EFM) is a technique similar to AFM. In this technique, the sample is grounded and a bias voltage is applied to the tip. The tip is still driven at near resonance frequency, but it is scanned over the sample at a higher altitude (30nm) than that used for AFM topographic imaging. Electrostatic interaction between the sample and the tip introduces a negative phase shift in the oscillation of the tip relative to the drive signal. In conducting regions, the biased tip will introduce a surface charge, which pulls the tip towards the sample causing the negative phase shift. Non-conducting regions do not display a surface charge and therefore, the tip does not interact with these regions. We expect graphite oxide to be electrically insulating, and EFM of graphite oxide on a Si/SiO_2 substrate confirms that this material is indeed insulating (Figure 4.1).

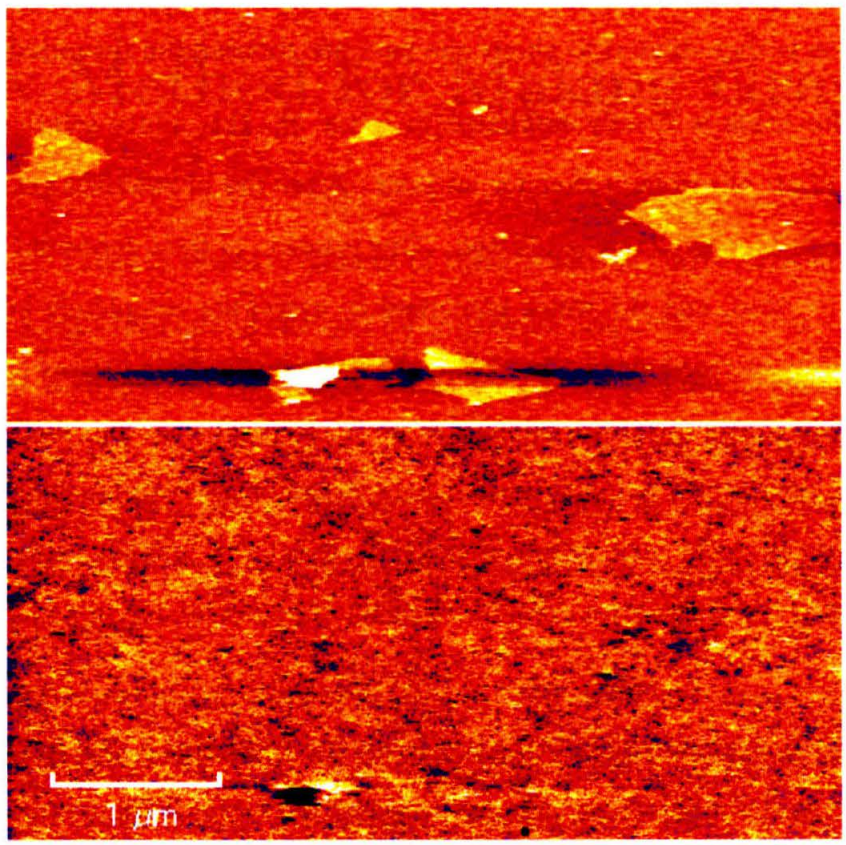

Figure 4.1: Graphite oxide on Si substrate. Flake height is about 1nm relative to substrate. Top image is AFM topography in tapping mode. Bottom image is EFM image of same area.

Having deposited the flakes, the next step is to reduce the graphite oxide back to graphene without removing it from the Si/SiO_2 substrate. To do this, the sample is annealed in Ar in a furnace for 30s-45s at 1025 °C, based upon the reduction technique present in Schniepp *et al.* [10]. After the annealing, EFM shows that the reduced material is electrically conductive (Figure 4.2). We have measured current-voltage curves for samples of this material prior to breakdown to determine the resistance of this material. For an annealing time of 30s, the electrical resistance is on the order of a GΩ, and when the sample is annealed for 45s this decreases to be on the order of a MΩ. Figure 4.3 shows current-voltage plots for graphite oxide annealed for 30s, and Figure 4.4 shows data from devices annealed 45s. Figure 4.5 displays the substantial difference in the magnitude of the conductivity of these two materials. Based upon these results, we think that it should be possible to find an annealing time at which this material is made substantially more conductive, to the point where it has a resistance on the order of kΩ and can substitute for graphene in our single molecule transistor devices. This is an area of continuing research.

The major benefit of reduced graphite oxide over traditional graphene, despite its currently higher electrical resistance, is that this material can be produced in bulk. Currently it is easily possible to find more than 5 candidate single-layer flakes per substrate, as the density of single-layer graphene flakes obtained using this method is fairly high. The limiting factor with this method is not the rate of production of the material, but the required AFM/SEM time necessary to characterize the flakes and make the electrodes. Consequently, if the issues of electrical resistance can be suitably resolved, this represents a significant step forward for the development of single molecule transistors with graphene electrodes.

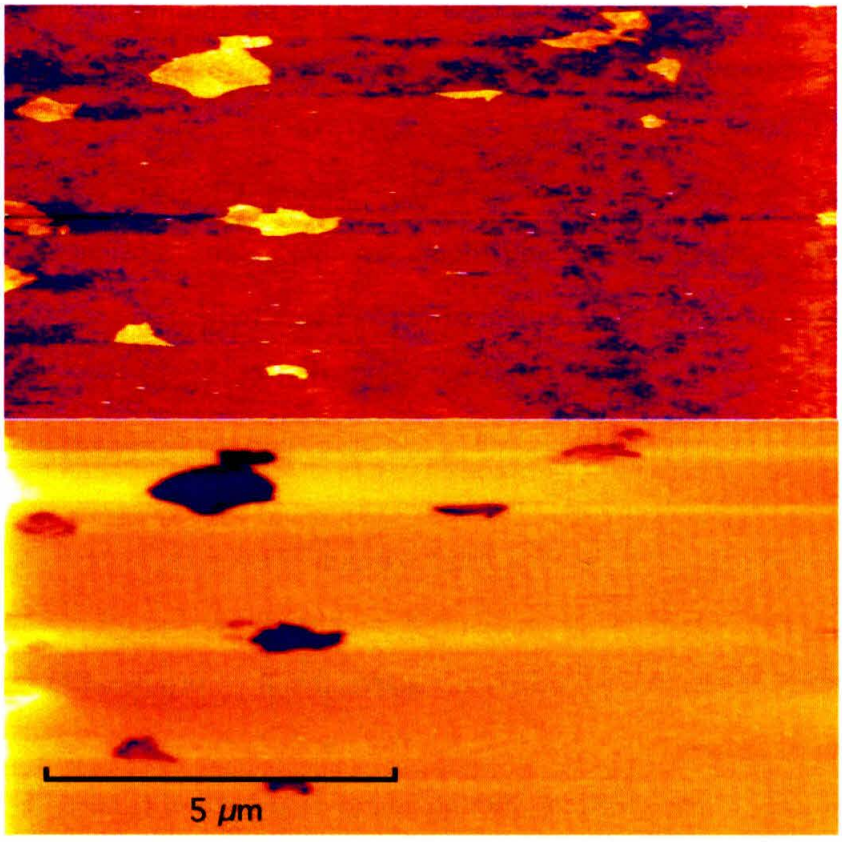

Figure 4.2: AFM micrograph of reduced graphite oxide on an Si substrate. Flake heights are all about 1nm relative to substrate. Top image is AFM topography in tapping mode. Bottom image is corresponding EFM image. Note large phase shifts indicating electrical conductivity.

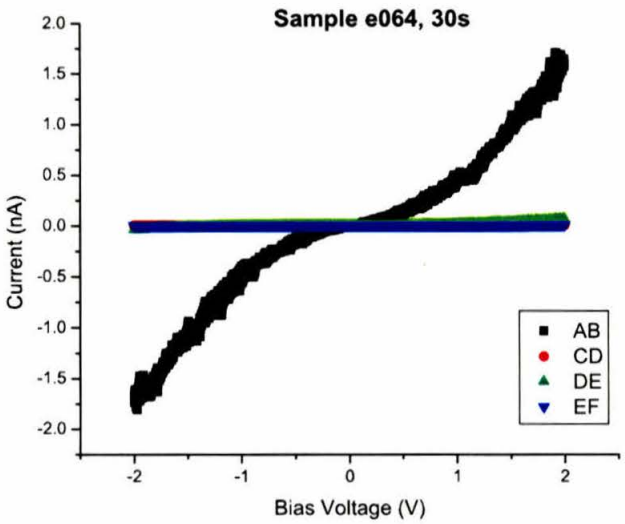

Figure 4.3: Current-voltage plots from four samples of graphite oxide after 30s of annealing at 1025°C.

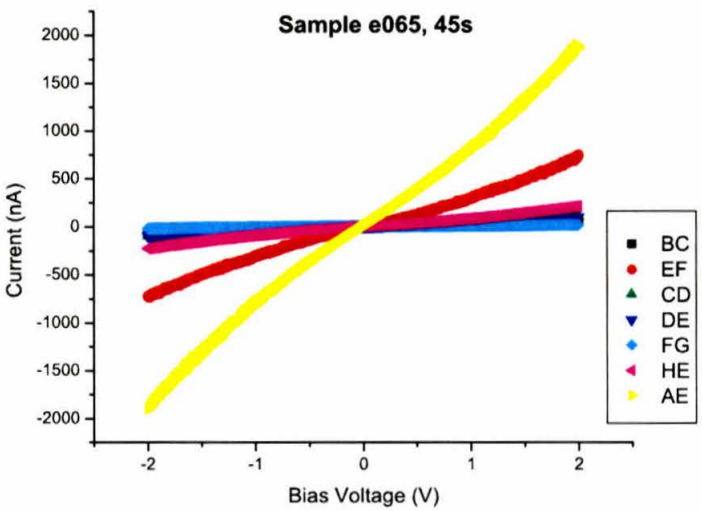

Figure 4.4: Current-voltage plots from seven samples of graphite oxide after 45s of annealing at 1025°C.

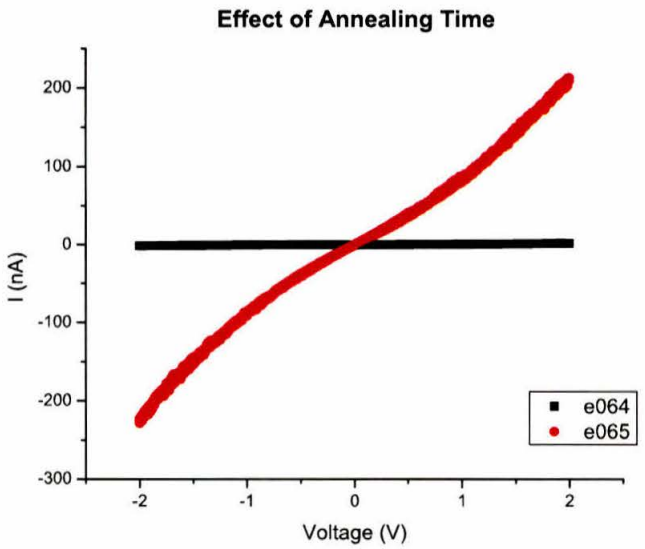

Figure 4.5: Sample HE from Figure 4.4 and sample AB from Figure 4.3. Note the substantial difference in magnitude of conductance between the best sample annealed 30s and an "average" sample annealed 45s.

Chapter 5

Capacitive Properties of Graphene

In addition to device fabrication and the development of a new method for making graphene, the capacitive properties of graphene samples were also studied in a brief experiment that used many of the same techniques already outlined in previous chapters. It is not completely understood how charge distributes itself on a single layer of graphene, which allows the possibility of interesting capacitive behavior. If we treat the graphene flake on the Si/SiO_2 substrate as a parallel plate capacitor, it is possible to test the uniformity of the charge distribution on graphene by looking at the screening of electric fields immediately above the flake, or outside the capacitor.

We begin by considering a net charge density per unit area of the graphene surface, denoted σ, which can be obtained by integrating the density of states,

$$\sigma = \int_0^\infty qD(E)f(E)dE \tag{5.1}$$

where $D(E)$ is the electronic density of states as a function of energy E and $f(E)$ is the Fermi function. For two-dimensional graphene, the electronic density of states including spin is given by

$$D(E) = \frac{2E}{\pi\hbar^2 v^2} \tag{5.2}$$

where v is the Fermi velocity in the material. Approximating at absolute zero, where the

Fermi function is simply a step function with value 1 between $E = 0$ and the Fermi energy E_F and 0 otherwise, we substitute (5.2) into (5.1) to get

$$\sigma = \frac{2q}{\pi\hbar^2 v^2}\int_0^{E_F} EdE = \frac{qE_F^2}{\pi\hbar^2 v^2} \tag{5.3}$$

.

Again approximating at absolute zero, we have that

$$\mu = E_F = \sqrt{\frac{\sigma 2\pi\hbar^2 v^2}{q}} \tag{5.4}$$

where μ is the chemical potential and we have substituted in the value for E_F obtained by rearranging (5.3). Since we are treating the graphene flake on the substrate as a capacitor, there is an electric potential $\phi = 4\pi\sigma d$ between the substrate and the flake from the surface charge, where d is the separation between the substrate and the graphene. Also present is the chemical potential from (5.4). Consequently, the total potential present is

$$V = 4\pi\sigma d + \sqrt{\frac{\sigma 2\pi\hbar^2 v^2}{q}} \tag{5.5}$$

which, given that $C = \frac{A\sigma}{V}$ by definition results in a total capacitance of

$$C = \frac{A}{4\pi d + \sqrt{\frac{2\pi\hbar^2 v^2}{q\sigma}}} \tag{5.6}$$

where A is the area of the graphene flake. In our treatment of the capacitance we have assumed that σ is uniform. However, if $\sigma(T)$ or $\sigma(V)$, the capacitance here will change as a function of these variables. If σ is small and non-uniform, it should be possible to see variation in the capacitance of the graphene-substrate system.

The experimental setup is illustrated in Figure 5.1. A graphene sample on an Si/SiO_2 substrate is placed in an AFM. The AFM tip resonance frequency ω_0 is measured but, unlike in previous experiments, the tip is not driven. A constant gate voltage is applied to

the substrate. In addition to this constant gate voltage, an oscillating voltage of constant amplitude and frequency ω_0 is applied to the substrate. A lock-in amplifier is set to measure the amplitude of oscillation of the AFM tip, as detected from the photodiodes, at the frequency ω_0. Since the AFM tip is not driven, any oscillation in the AFM tip is caused by interaction between the tip and image charges in the graphene arising from the applied electric potential. The stronger the interaction between the tip and the sample, the larger the amplitude of AFM tip oscillation.

The AFM tip scans the same linear region of the sample repeatedly. For each scan, the substrate gate voltage is increased incrementally, ultimately ranging from -10V to 10V. The resulting image (Figure 5.2) contains information about the tip's linear position, applied gate voltage, and interaction with the sample. Figure 5.2b shows the voltage data from the lock-in amplifier in the color scale, with zero amplitude corresponding to black on the color scale. We can analyze the interaction strength as a function of applied bias voltage. If this deviates from linear, we are seeing the variation in capacitance due to variation in σ, as illustrated in Equation (5.6).

From Figure 5.2c, it is clear that the interaction strength varies linearly with the voltage. It seems that the signal from the substrate overwhelms any signal that may be observed above the graphene flake and that the graphene uniformly screens the electric field. This may be due to a low σ in graphene or the effect may be thermally suppressed in ambient laboratory conditions. It might also be that doping of the graphene by atmospheric H_2O vapor changed the conductive properties of this material, suppressing the anomalous capacitance. There is also the possibility that the graphene in this sample was not single layer.

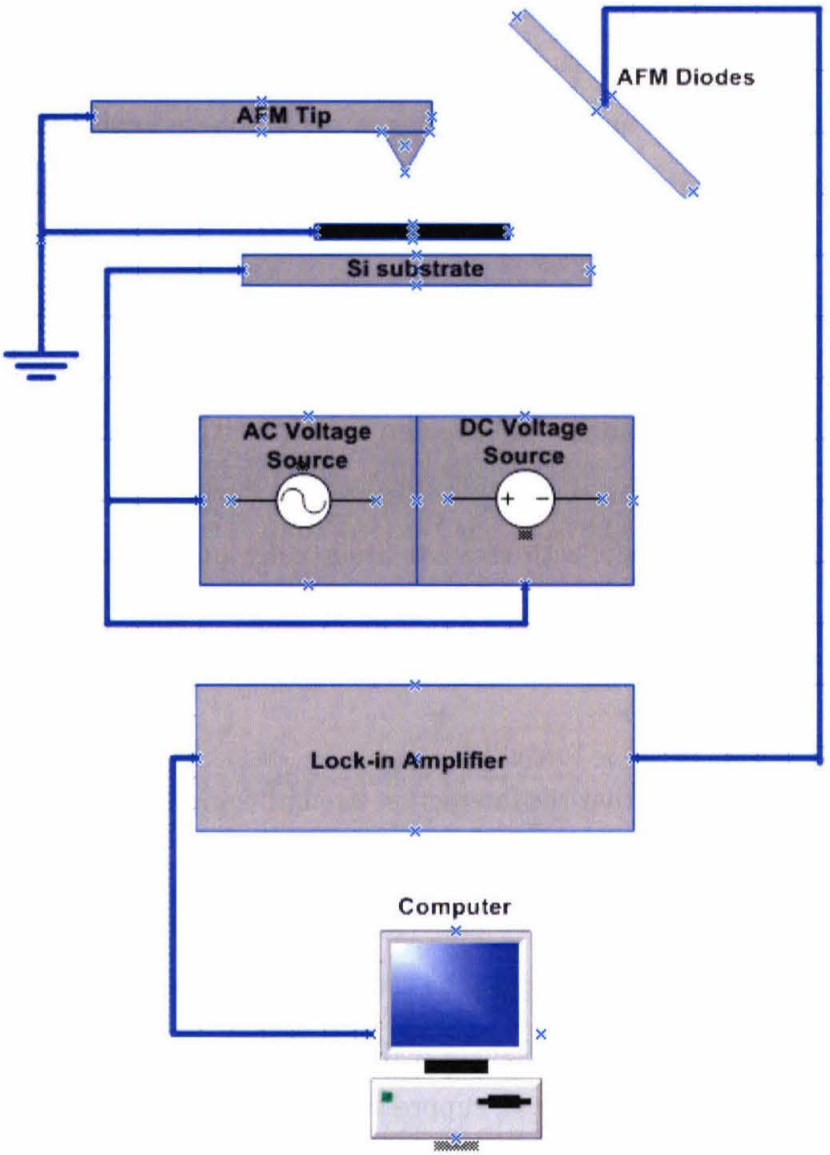

Figure 5.1: The experimental setup for the AFM capacitance experiment.

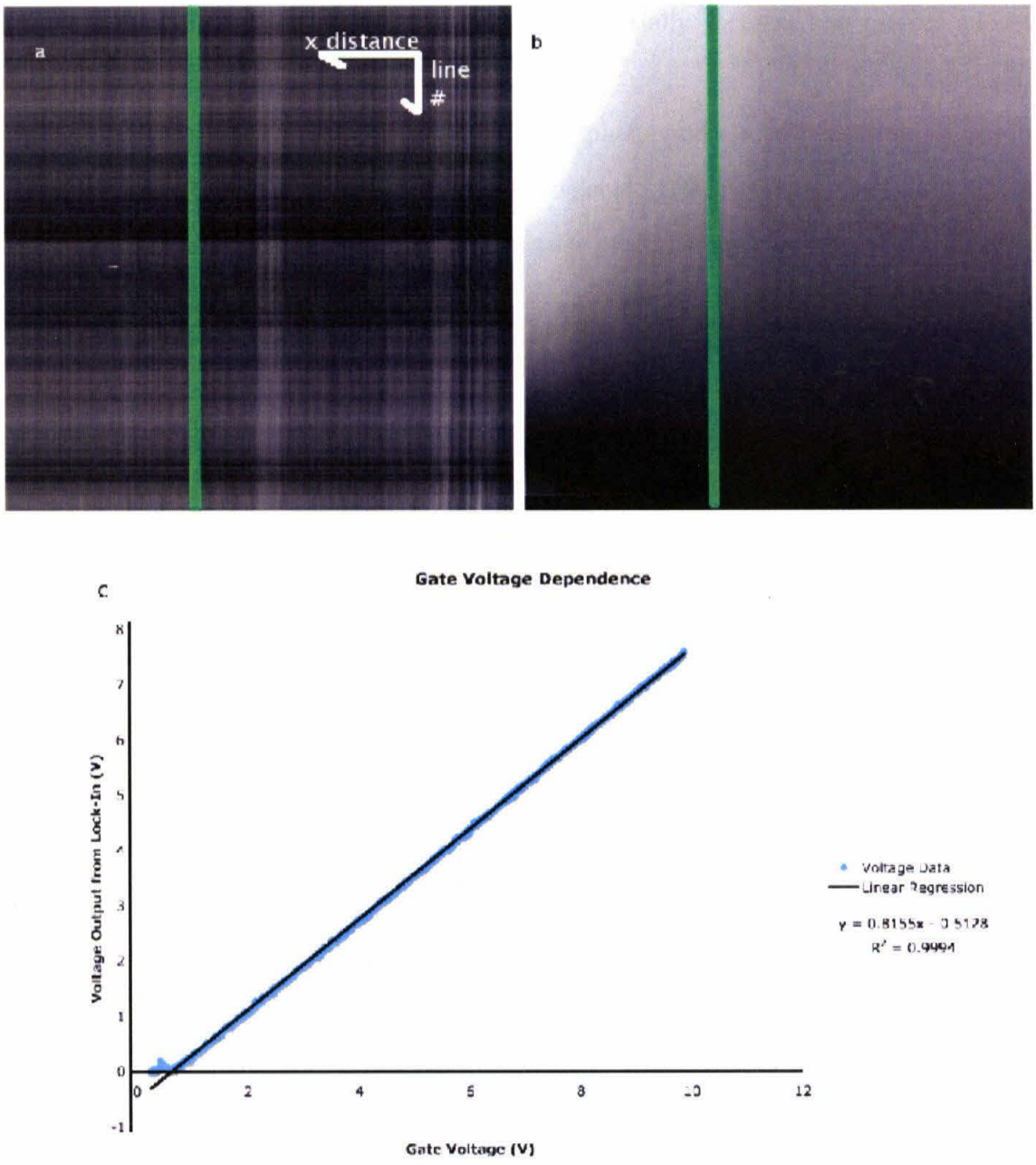

Figure 5.2: Data from the AFM capacitance experiment. a) Topographic data for the scanned line. Horizontal distance is on the image x axis and subsequent horizontal scans are displayed on the image y axis. b) Data from the lock-in amplifier indicating the strength of the interaction. For this image, gate voltage decreases from 10V at the top of the image to 0V at the bottom. c) Data from one vertical section of this image, indicated by a green line in a) and b). Gate voltage is on the horizontal axis and lock-in output voltage is on the vertical axis.

Chapter 6

Conclusions and Future Directions

In this thesis, we have presented initial results related to the development of single molecule transistors with graphene electrodes. Specifically, we have shown that it is possible to build the necessary structures – contact electrodes and the nanogap – with graphene, and we have begun to actually attempt measurements with these devices.

One of the technical difficulties limiting the further development of these single molecule transistors was the absence of a high-throughput method for the production of graphene, substantially limiting the rate of device production. However, we have shown that is possible to recover electrical conductivity in single-layer samples through the reduction of graphite oxide. Since graphite oxide exfoliates easily in water, this technique produces a high density of single-layer samples per substrate, and if the electrical conductivity can be improved through adjustment of the annealing process, this could prove to be a reliable source of artificial graphene.

Further work must still be done with the annealing process of graphite oxide, to determine the annealing time that optimizes the electrical resistance of the reduced material. It might also be possible to perform this reduction with chemical techniques, as one other group at the APS March Meeting are attempting to do.

Further research is also required to understand the electromigration breakdown process, in an attempt to improve the success rate of the breakdown. If the mechanism could be

understood and better controlled, this could substantially increase the rate of successful device production.

When the issues surrounding production of graphene and electromigration are resolved, it then becomes possible to use these single molecule transistors at their full potential, exploring the interesting physics of both molecular orbital energy levels and dimensionality in the Kondo effect.

Bibliography

[1] Novoselov, K. S. *et al.*(2004). *Science* **306**, 666-669.

[2] Zhang, Yuanbo *et al.*(2005). *Nature* **438**, 201-204.

[3] Novoselov, K. S. *et al.*(2006). *Nature Physics* **2**, 177-180.

[4] Liang, Wenjie *et al.*(2002). *Nature* **417**, 725-729.

[5] Park, Hongkun *et al.*(2000). *Nature* **407**, 57-61.

[6] Novoselov, K. S. *et al.*(2005). *PNAS* **102**, 10451-10453.

[7] Ferrari, A. C. *et al.*(2006). *arXiv* cond-mat/0606284v1.

[8] Stankovich, Sasha *et al.*(2006). *Nature* **442**, 282-286.

[9] Stankovich, Sasha *et al.*(2006). *J. Mater. Chem.* **16**, 155-158.

[10] Schniepp, Hannes C. *et al.*(2006). *J. Phys. Chem B.* **110**, 8535-8539.

[11] Hummers, William S. and Richard E. Offeman (1958). *J. Amer. Chem. Soc.* **80**, 1339.

[12] Image from `http://en.wikipedia.org/wiki/Image:Single_electron_transistor.svg`, last viewed 4/13/07.

[13] Ferry, David K. and Stephen M. Goodnik (1997). *Transport in Nanostructures.* Cambridge, UK: Cambridge University Press, 226-249.

[14] Jarillo-Herrero, Pablo *et al.*(2004). *Nature* **429**, 389-392.